

An Abstract of the Thesis of

Fa-Tai Tang for the Degree of Master of Science in Chemistry
(analytical) presented on April 21, 1983.

Title: The Diffusion Coefficient of Propane in Helium

Abstract approved: **Redacted for Privacy**
Dr. Stephen J. Hawkes

A specially designed gas chromatograph with both TCD and FID has been tested for the measurement of the diffusion coefficients of methane and propane in helium. Knox's arrested elution technique⁽⁴⁾ was used and yielded a value of 0.6431 cm²/sec averaged with the value obtained by Yang and Hawkes⁽⁷⁾. Values of the binary molecular diffusion coefficient for propane in He were obtained at atmospheric pressure over the temperature range from 21.3 to 60.3°C. The data fitted the equation $\log D_{12} = -8.1277 + 3.0805 \log T$ with correlation coefficient of 0.9976.

The Diffusion Coefficient
of
Propane in Helium

by
Fa-Tai Tang

A THESIS
submitted to
Oregon State University

in partial fulfillment of
the requirements for the
degree of
Master of Science
Completed April 21, 1983
Commencement June 1983

Approved:

Redacted for Privacy

Professor of Analytical Chemistry in charge of Major

Redacted for Privacy

Chairperson of Chemistry Department

Redacted for Privacy

Dean of Graduate School

Date thesis is presented: April 21, 1983

Typed by Jane L. Jarvi for Fa-Tai Tang

Acknowledgements

My sincerest thanks go to Professor Stephen J. Hawkes for his advice, encouragement, patience and practice during the course of the project; I will be forever indebted to him.

Thanks is also given to the Institute of Nuclear Energy Research, Atomic Energy Council, R.O.C. which supported me financially in my Master of Science studies at Oregon State University.

I am eternally grateful to my parents, my wife Yeh-Chiao, and to my son Jin-Ho, whose support and encouragement has been the constant help throughout the course of my education.

Table of Contents

I. Introduction	1
II. Theory	4
A. Background	4
B. Causes of Error.	5
III. Experimental Work.	15
A. Construction of the Apparatus.	15
B. Operation of the Apparatus	25
IV. Results and Discussion	28
V. Conclusions.	34
 Bibliography	 35
Appendices	
Appendix A: The Operation of Computer Interface	36
Appendix B: Fortran Program for the Correction of the Time Base, Output Signal and the Calculation of Sample Peak Statistics	41
Appendix C. Control Language for Calling BMDP-AR and the Subroutine of the Fit Equation.	43
Appendix D: A Sample of the Computer Output for Fitting Concentration Profile and Obtaining D_{12}^*	46

List of Figures

<u>Figure</u>		<u>Page</u>
1.	Effect of Input Distribution	11
2.	The Shape of Input Distribution for Arrested Elution . .	16
3.	Flow Diagram of Gas Chromatography System.	17
4.	Exploded View of Flame Ionization Detector	20
5.	Detector Base.	21
6.	Assembled View of Detector	22
7.	Stream Splitter.	23
8.	$-\text{Log } D_{12}^*$ vs. $\text{Log } T$ for the C_3H_8 -He System	32

List of Tables

<u>Table</u>		<u>Page</u>
I	Binary Molecular Diffusion Coefficient (CH_4 -He).	29
II	Binary Molecular Diffusion Coefficient (C_3H_8 -He)	31
III	Comparison of Experimental and Calculated Diffusion Coefficients (C_3H_8 - He)	33

THE DIFFUSION COEFFICIENT OF PROPANE IN HELIUM

I. Introduction

The gaseous binary molecular diffusion coefficient D_{12} is an important physical parameter in many areas of both basic and applied research since it plays an important role in chemical reactions and has to be considered in the design of distillation columns. Diffusion also plays a major role in peak broadening in chromatography and accurate values of diffusion coefficients are necessary in the testing of chromatographic theory.

There are various theoretical and experimental methods employed for their measurement and a lot of reports published since the early years of the century. However, the results obtained from different researchers have always deviated to some extent from each other and the experimental measurement is time-consuming. It is the object of the research to explore the possibility of obtaining highly precise and accurate diffusion coefficients by a specially designed Gas Chromatography system, and by employing a microcomputer for accurate data collection and for least squares fitting of the theoretical zone dispersion equation.

There are two experimental approaches, Giddings' continuous elution method⁽¹⁻³⁾ and the arrested elution method⁽⁴⁾. The continuous elution method for the determination of D_{12} is generally conducted in an open tube with circular cross section. The average carrier stream velocity is chosen such that the zone dispersion depends

principally on only one of the terms in the Taylor equation⁽⁵⁾ - the longitudinal diffusion term. The advantage of this method is that the speed of data collection is very rapid and the precision is comparable to or even better than most of the other methods used so far. However, an inherent weakness of the method is that zone broadening factors such as racetrack, secondary flow, etc., can not be isolated in the same run of the experiment because the column is long and because the result is greatly affected by slight errors in the estimate of the radius or from the roughness of the wall. In this experiment, the approach was the arrested elution method pioneered by Knox and McLaren⁽⁴⁾, modified by Yang, Hawkes and Lindstrom⁽⁶⁾ and further modified for this thesis. This method was basically the same as the continuous elution method except the carrier flow was arrested when the solute zone had migrated about half-way along the column. The solute zone was then allowed free molecular diffusion for a period of time, and then eluted from the column by resuming the carrier flow. The following advantages of using the arrested elution method were given by Knox and McLaren. (1) The effects of zone broadening other than axial molecular diffusion and non-uniform flow profile do not affect the result. So, the end effect correction as mentioned in the continuous elution method is not necessary. (2) The column can be very short and hence decrease the possible error introduced by the pressure drop between the inlet and outlet of a long column, especially a packed column. (3) No assumptions are made about the precise form of the flow profile, the smoothness of the column wall or the accuracy with which the column diameter is known. But the disadvantage of the method is that a constant velocity must be maintained over a long period for runs at various arrested times and,

with traditional methods of measuring variance in calculating D_{12} , a Gaussian elution peak is assumed. Experimentally, a near Gaussian elution peak may be obtained but a constant velocity over a period of about 3 hours is hard to obtain. The need for several runs to get a D_{12} value may degrade the advantage of employing GC as a rapid method in determining D_{12} values.

Therefore the advantages of the above-mentioned method can be obtained only if a single run of the experiment will be sufficient for the measurement of a D_{12} value with high precision and accuracy. This may be achieved by a direct least-squares fit of the experimental data to the theoretical equation of the eluted concentration profile and computing the D_{12} values. This method also has the additional advantage that any deviations from the expected form of the concentration profile give warning⁽⁶⁾ of the incorrect design of the experiment or malfunction of the equipment. However, the use of a single run degrades some of the advantages of Knox and McLaren's method. They used several arrested times for each sample and found D_{12} from the slope of a plot of dispersion against time. In a single run the equation used must describe accurately the effect of the inlet distribution, the shape of the tube, and the flow profile. Careful engineering and rigorous mathematics are necessary.

At first we check whether the design of the GC system is correct by measuring the diffusion coefficient D_{12} of methane. Then the diffusion coefficients of propane at temperature from 21.3° to 60.3°C are obtained.

II. Theory

A. Background

The theoretical expression for solute zone dispersion in a tube of open circular cross section can be obtained by solving the mass balance equation. It had been derived by Dr. Lindstrom in reference 7. The equation is written as:

$$C(L, t) = \frac{C_0 \left[\left(\frac{D_{12}^*}{P_0} + \frac{r^2 v^2 P_0}{48 D_{12}^*} \right) + v t_2 \frac{D_{12}^*}{P_0} \right]}{2 \sqrt{\pi} \left[\left(\frac{D_{12}^*}{P_0} + \frac{r^2 v^2 P_0}{48 D_{12}^*} \right) t_m + t_2 \frac{D_{12}^*}{P_0} \right]^{3/2}} \times \exp \left(\frac{-(L - v t_m)^2}{4 \left[\left(\frac{D_{12}^*}{P_0} + \frac{r^2 v^2 P_0}{48 D_{12}^*} \right) t_m + \frac{D_{12}^* t_2}{P_0} \right]} \right) \quad (1)$$

where: C_0 = the initial concentration

L = the length of the column

D_{12}^* = molecular diffusivity at one atmosphere

P_0 = the output pressure in atmospheres

r = the radius of the column

v = the velocity of the carrier gas

t_2 = the arrested time

t_m = the time spent mobile

By measuring the concentration profile of the dispersed zone at the end of the column, and then fitting these data to the Eq. 1, the binary molecular diffusion coefficient at 1 atm, D_{12}^* , can be obtained.

The equation incorporates Taylor's equation⁽⁵⁾:

$$D_{eff} = D_{12} + r^2 v^2 / 48 D_{12}$$

D_{eff} = effective dispersion

r = the radius of the column

v = the velocity of the carrier gas

D_{12} = the axial diffusion

the first term of Taylor's equation tacitly assumes that there is no adsorption on the column wall, which is reliable in our work. The second term assumes that the tube is perfectly circular and that the walls are perfectly smooth so that the flow profile is perfectly parabolic. It is necessary to use a slow enough flow rate that the second term is so small a fraction of the first that errors in these assumptions are negligible.

B. Causes of Error

The precision and accuracy of the data obtained from this method depend on the extent of the contribution to the zone broadening due to zone-broadening factors, not included in the Equation 1 (such as secondary flow, the racetrack effect, and end effects). Failure in this experimental design is easily detected because it gives rise to systematic deviation of the experimental data from the fitted equation at the tails and the maximum of the peak. In the following some important causes are discussed.

Secondary Flow

For an ideal fluid in a laminar flow within a curved column of any cross section, secondary flow may be introduced due to the pressure

gradient developed across the bend because of the centrifugal force of the fluid moving around the bend. The fluid in the central streamlines is subjected to relatively greater centrifugal force because of its greater axial velocity. The fluid near the center is therefore thrown outward toward the outer wall of the bend. Since the fluid is continuous, it is continuously replaced by the recirculation of fluid along the walls. The net result is the establishment of the spiral motion of secondary flow in a curved column.

In a chromatography column, the secondary flow effect in contrast to most of the known zone-broadening factors is to enhance the zone dispersion across the cross-sectional plane, and hence minimize the axial zone broadening. A narrower peak would be expected from a strong effect of secondary flow superimposed on the elution peak.

Secondary flow may be indicated by the extra pressure drop, Δp , across the curved column in comparison with the pressure drop across the straight tube with the same geometry. The larger the pressure drop, the higher the secondary flow effect. This extra pressure drop, Δp , may be expressed as

$$\Delta p = (F-1) \frac{8\eta Lv}{r^2} \quad (2)$$

where η is the viscosity of the carrier gas in the column and F is the resistance factor which was shown by White⁽⁷⁾ as

$$F = 1 \text{ for } K \leq 11.6 \quad (3)$$

and

$$1/F = 1 - [1 - (11.6/K)^{0.45}]^{1/0.45} \text{ for } K > 11.6 \quad (4)$$

where K is Dean's factor which was given as

$$K = \frac{2\rho v r}{\eta} \left(\frac{2r}{D} \right)^{\frac{1}{2}} \quad (5)$$

ρ is the density of the carrier gas in the column, and D is the radius of the curvature of the coil.

Equation 3 indicates the upper limit of K where secondary flow effect does not occur. Equation 5 can be used to estimate the upper limit of flow rate, v , that can be used without the introduction of the secondary flow, for a given carrier gas, radius of curvature, radius of the column, and the temperature of the fluid. For example, the estimated upper flow rate of carrier helium can be as high as 273 cm/s at 60°C with a radius of curvature of 10 cm and a radius of 0.2184 cm before the secondary flow effect must be considered. Generally the secondary flow effect can be neglected if a sufficiently large radius of curvature of the column and a low density fluid are employed. In this experiment, the flow rate is no more than 3.7 cm/s. So, the secondary flow effect can be neglected.

Giddings Racetrack Effect

In the case of coiled columns the velocity of the flow near the inside is higher than that near the outside because both experience the same pressure gradient but different flow path lengths due to coiling. This leads to a nonequilibrium laterally across the column. For high precision work, the Giddings' racetrack effect has to be evaluated.

For an open circular cross-sectional coiled column the additional zone broadening, in terms of the height equivalent to a theoretical plate, due to this racetrack effect may be expressed as⁽⁸⁾

$$H_{\text{coil}} = \frac{7vr^4}{12D_12D^2} \quad (6)$$

The equation shows the dependence of H_{coil} on the secondary power of (r^2/D) . It indicates that we can minimize the racetrack effect simply by decreasing the ratio (r^2/D) and flow rate. The coil as mentioned in the previous case is able to contribute the extra plate height, H_{coil} , by less than 0.0001 cm at the flow rate of 272 cm/s for propane. Since in this work the flow rate is no more than 3.7 cm/s, the contribution from the racetrack effect is negligible.

End Effects

Some of the most important causes of zone broadening occur outside the column. For example, the volume occupied by a sample as it enters the column gives it an initial value of σ^2 which may not be negligible. Generally the end effects include the zone broadening from the finite volume of the injection port, the detector volume and the dead volume due to connecting tubing pockets, etc.

Indeed the end effects are the most important extra zone broadening factor in GC systems. Appreciable end effects will skew the eluted peak and the efficiency of separation is reduced. Giddings and Seager⁽³⁾ provide a method for the correction of the end effect. However, as mentioned earlier, the experimental exercise is difficult for a normal GC system and routine operation. In this work we measure the input distribution and correct for it by a variant of Giddings and Seager's method and make other end effects negligible by careful apparatus design. We then compare the D_{12}^* value of methane in He with that obtained by Hawkes and Yang⁽⁹⁾. Identical D_{12}^* should be obtained

if the zone dispersion is due only to axial molecular diffusion and the effect of nonuniform flow profile.

Gas Compressibility Effect

In GC systems the gas expands as it proceeds along the column because of the pressure drop. As it expands the linear velocity increases and so does D_{12} . However, v is usually determined by dividing the column length by the mobile time of the sample in the column and is usually designated \bar{v} . The D_{12}^* must therefore be calculated at the average pressure \bar{p} . James and Martin⁽¹⁰⁾ have shown that this is related to the outlet pressure by

$$\bar{p} = P_o^j \quad (7)$$

$$j = 3(P_i^2/P_o^2 - 1)/2(P_i^3/P_o^3 - 1)$$

where P_i is the inlet pressure and P_o is the outlet pressure.

Meanwhile, an increment of σ^2 introduced by the first part of the column expands through the remainder of the column, but an increase of σ^2 introduced when the zone passes through the last part of the column is not further expanded. Gidding⁽¹¹⁾ has shown that this requires all gas phase dispersion terms to be multiplied by a factor f defined by

$$f = \frac{j^2(P_i^2/P_o^2 + 1)}{2} \quad (8)$$

In this experiment the pressure drop between inlet and outlet is 0.001 psi. So, the gas compressibility effect can be neglected.

Effect of Input Distribution

In practice, the delta function input distribution which has been assumed throughout is unattainable, since the vapor and the sample injector cavity occupy a finite volume. In accurate work it is necessary to consider it. Two extreme kinds of possible input distribution have been recognized by Porter, et al.⁽¹²⁾. The first extreme is that in which complete mixing occurs in the sample injector cavity, so that the input distribution is of the Poisson type (Figure 1-a). There is no simple formula to correct the extra zone broadening from this cause. In the second extreme, it is assumed that the input solute enters into the column as a compact plug of finite volume within which there is a uniform concentration. The effect of non-ideal linear chromatography upon such an input distribution is to superimpose a Gaussian distribution upon the plug of the solute. The resulting output distribution is shown in Figure 1-b. In this experiment the input distribution is very close to the second extreme. The output distribution is illustrated in Figure 1-c. Therefore we can correct the measured diffusion coefficient according to the following:

$$\sigma^2_{\text{meas}} = \sigma^2_{\text{col}} + \sigma^2_{\text{input}} \quad (9)$$

$$2D_{\text{meas}}t = 2D_{\text{true}}t + \sigma^2_{\text{input}} \quad (10)$$

where t is total time of elution, D_{true} is the true D_{12} and D_{meas} is the fitted D_{12} . For square plug input,

$$\sigma^2_{\text{input}} = L^2/12 \quad (11)$$

Substituting Equation 11 into Equation 10

$$2D_{\text{meas}}t = 2D_{\text{true}}t + L^2/12 \quad (12)$$

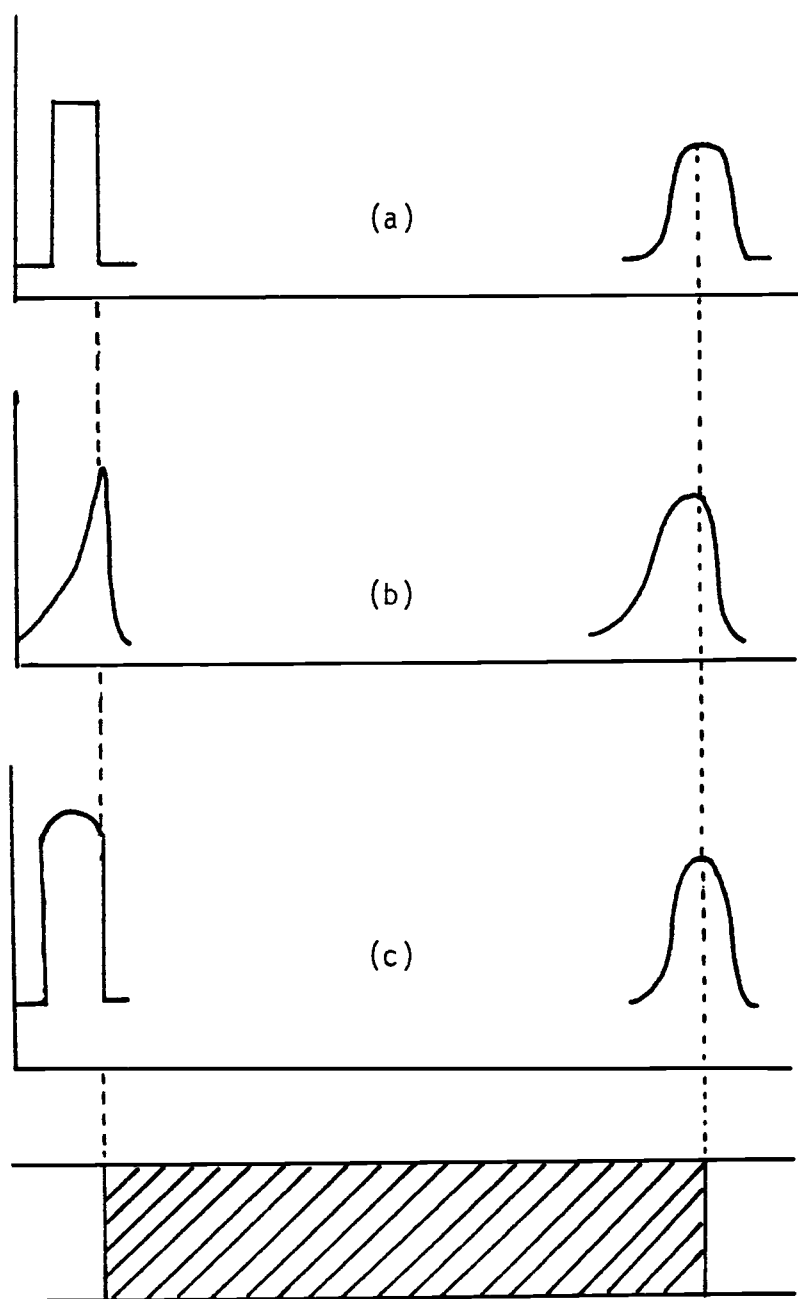


Fig. 1 effect of input distribution

(a) plug type input distribution

(b) poisson type input distribution

(c) the input distribution in this experiment

Equation 12 is divided by $2t$

$$D_{\text{meas}} = D_{\text{true}} + L^2/24t \quad (13)$$

Effect of Sample Size

In the column the total pressure inside a zone is the same as the total pressure elsewhere (neglecting the over-all pressure gradient). Since the zone is not infinitely small, the partial pressure of carrier gas must be correspondingly reduced. Because the mass flow rate of carrier gas in the column must remain constant along its path, it follows that the carrier velocity is greater inside the zone than elsewhere, particularly in those parts of the zone where the concentration is high. This effect makes the center of the zone move more rapidly through the column than the other parts, so that it becomes skewed towards the end of the column, and so that a slightly asymmetry is imposed upon the peak.

The skewness of the peak is defined as

$$z_1 = \frac{m_3}{m_2^{3/2}} \quad (14)$$

where $m_k = \sum_{i=1}^n (t_i - \bar{t}_p)^k f(t) \quad (15)$

$$\bar{t}_p = \sum_{i=1}^n t_i f(t) \quad (16)$$

$$f(t) = \frac{V}{\sum_{i=1}^n V_i} \quad (17)$$

V = the output voltage from detector at any instant.

$f(t)$ = the frequency distribution at any instant

m_1 = mean elution time

m_2 = the time base variance of the peak.

The negative value of skewness indicates peak fronting and positive value indicates peak tailing. Brubner⁽¹³⁾ gives a complex expression relating skewness to column constants. We have not fitted our data to it because Yang⁽⁶⁾ showed that the fit to Equation 1 is sufficient to show whether the apparatus is operating satisfactorily.

Effect of Detector and Readout System

The effects of the detector and readout system on peak shape and retention can be separated into three groups: (1) non-linear response to concentration (2) internal detector geometry and (3) slow response due to time constant.

Almost all detectors respond linearly to concentration over only a limited concentration range. But the FID was found to be less than perfectly linear. The slope of the least square fit straight line obtained from the data points is 0.99⁽¹⁴⁾. This means that

$$S \propto C^{0.99} \quad (18)$$

where S is the output voltage and C is concentration. Because data was always taken from the top half of the peak, the signal covered only a range of two, so that this effect can be neglected.

Detector geometry involves sudden changes in cross section, causing spreading and tailing. In this experiment it will not happen because the capillary tube connecting the FID jet and the column extended 1.5 in. into the column. Another different geometrical factor is due to the fact that there is a finite volume of gas in contact with

the sensing element. Therefore, at any instant time the detector registers a concentration integrated over the solute within the sensing volume. But it can be neglected in the FID because the cross-section is very small.

The detector and amplifier connected to it take a finite time to respond to a signal presented to them. As a result of the slow response the chromatogram does not faithfully represent the concentration profile reaching the detector. So the observed peak has its centre of gravity and maximum amplitude delayed, its height reduced and its width and tailing increased.

The errors produced are clearly related to the ratio of the time constant τ to the peak width. In this work $\tau/W_{1/2}$ is less than 0.01. A table by Dr. Piepmeier⁽¹⁵⁾ shows that when $\tau/W_{1/2}$ is 0.020, the ratio of σ^2 observed to true σ^2 is 1.002. For propane at 60°C, this would make an error of $0.002 \times 0.4365 = 0.0009$ in D_{12} . Since $\tau/W_{1/2}$ in this work is less than half the lowest value, 0.020, in Dr. Piepmeier's table, the error in D_{12} is negligible.

III. Experimental

The specially designed gas chromatograph is equipped with a thermal conductivity detector and a flame ionization detector. From the output of thermal conductivity detector the top part of the peak (shown in Figure 2) could be cut into the second main column for the arrested elution. In comparison to other GC systems, this one has the following advantages: (1) it is easy to maintain, (2) the input distribution is very close to the compact plug and easily corrected, and (3) it could give warning of the malfunction of the equipment. The flow diagram is given in Figure 3.

A. Construction of Apparatus

Detector

The Carle Model 100 Micro-Thermal Conductivity detector is employed to measure the input distribution of the sample. The Model 100 system consists of a miniaturized, full flow, dual thermistor detector and a control unit which is composed of an advanced bridge circuit, broad range, high resolution controls and a simple power supply of eight mercury reference cells.

At the end of the column the concentration profile of the eluted peak was detected by a flame ionization detector system. Commercial FID's are unacceptable from several standpoints. First, they all have long insulated signal conductor cables which increases the input capacitance of the measurement system and its response time. Second,

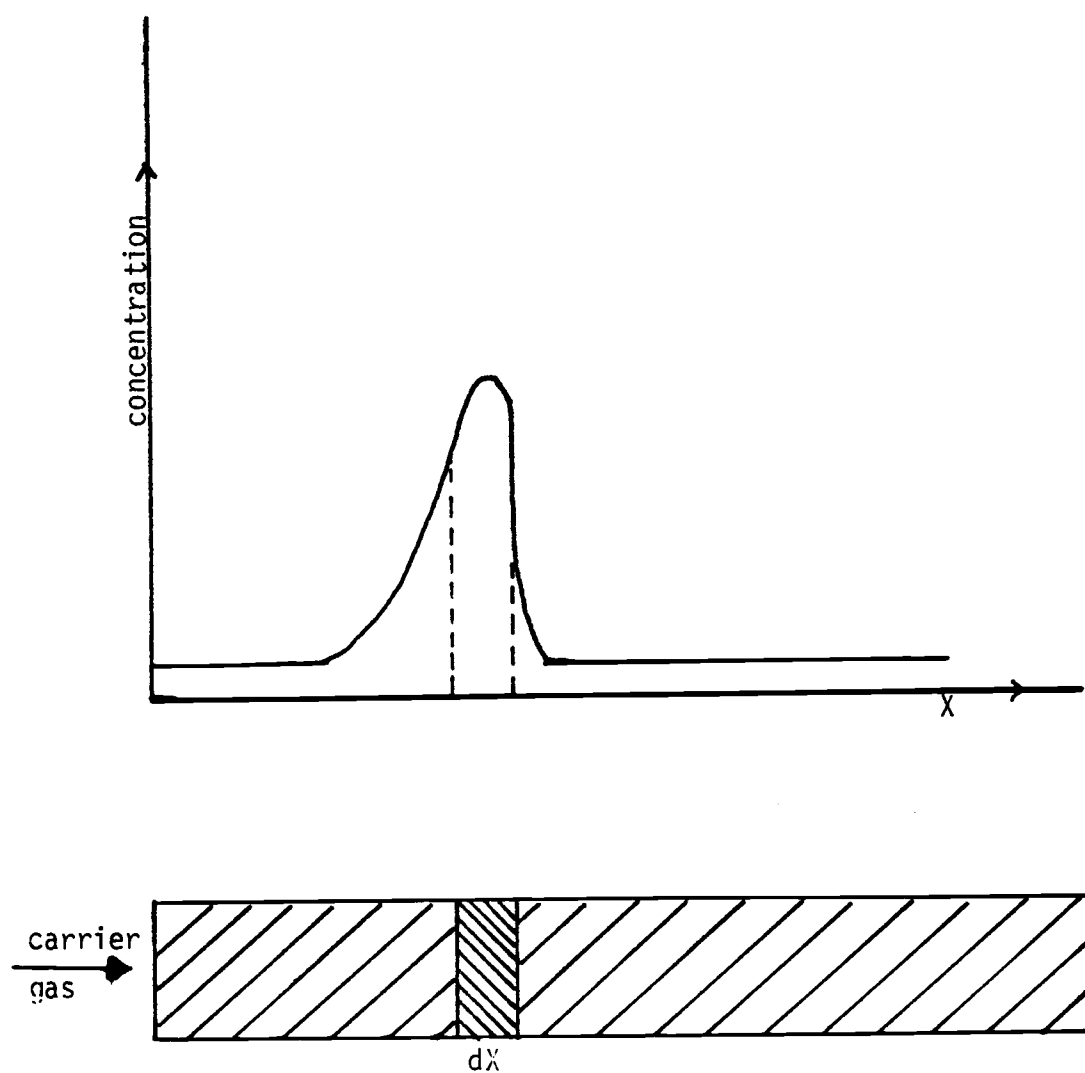


Fig. 2 the shape of input distribution for arrested elution

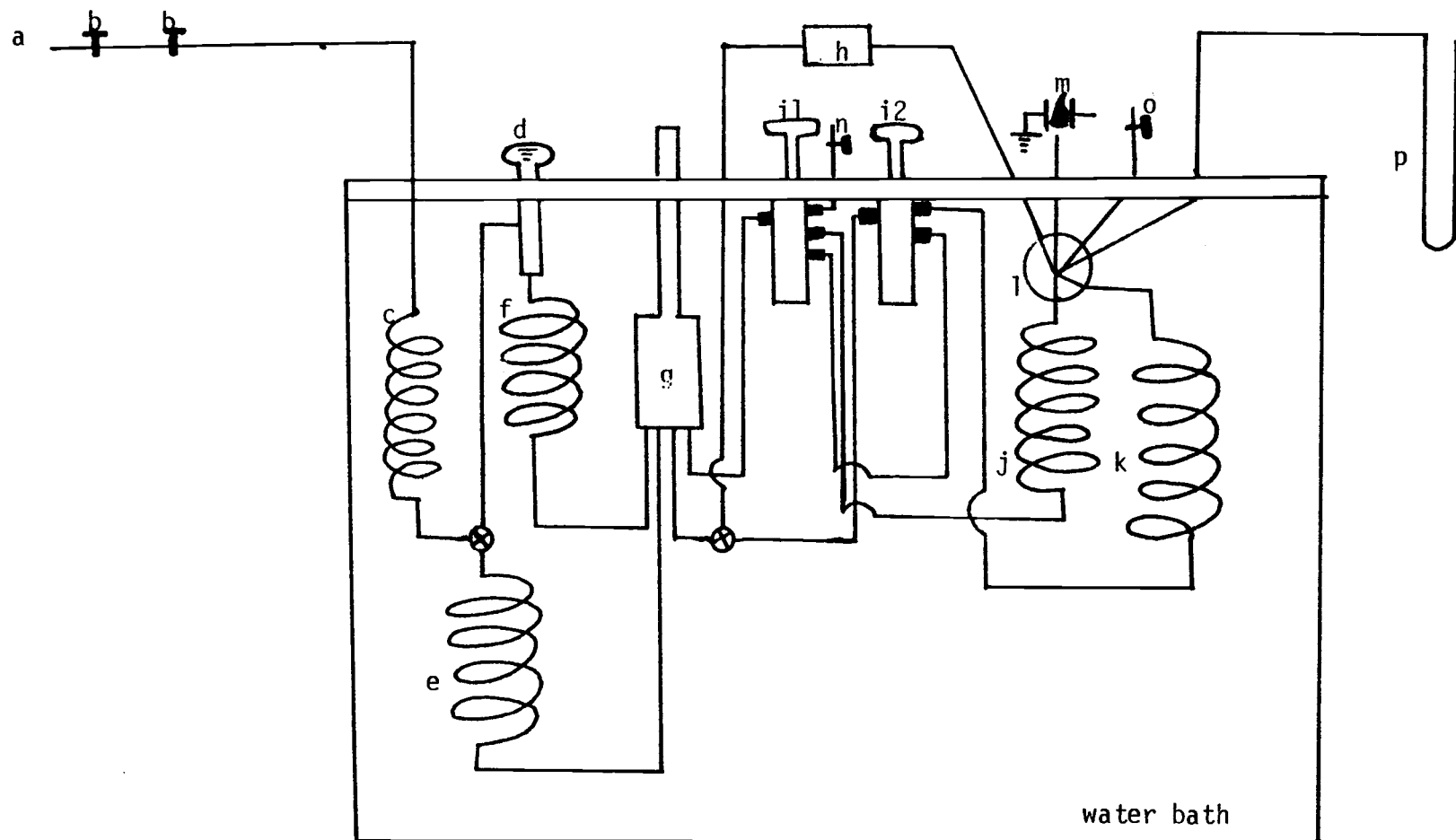


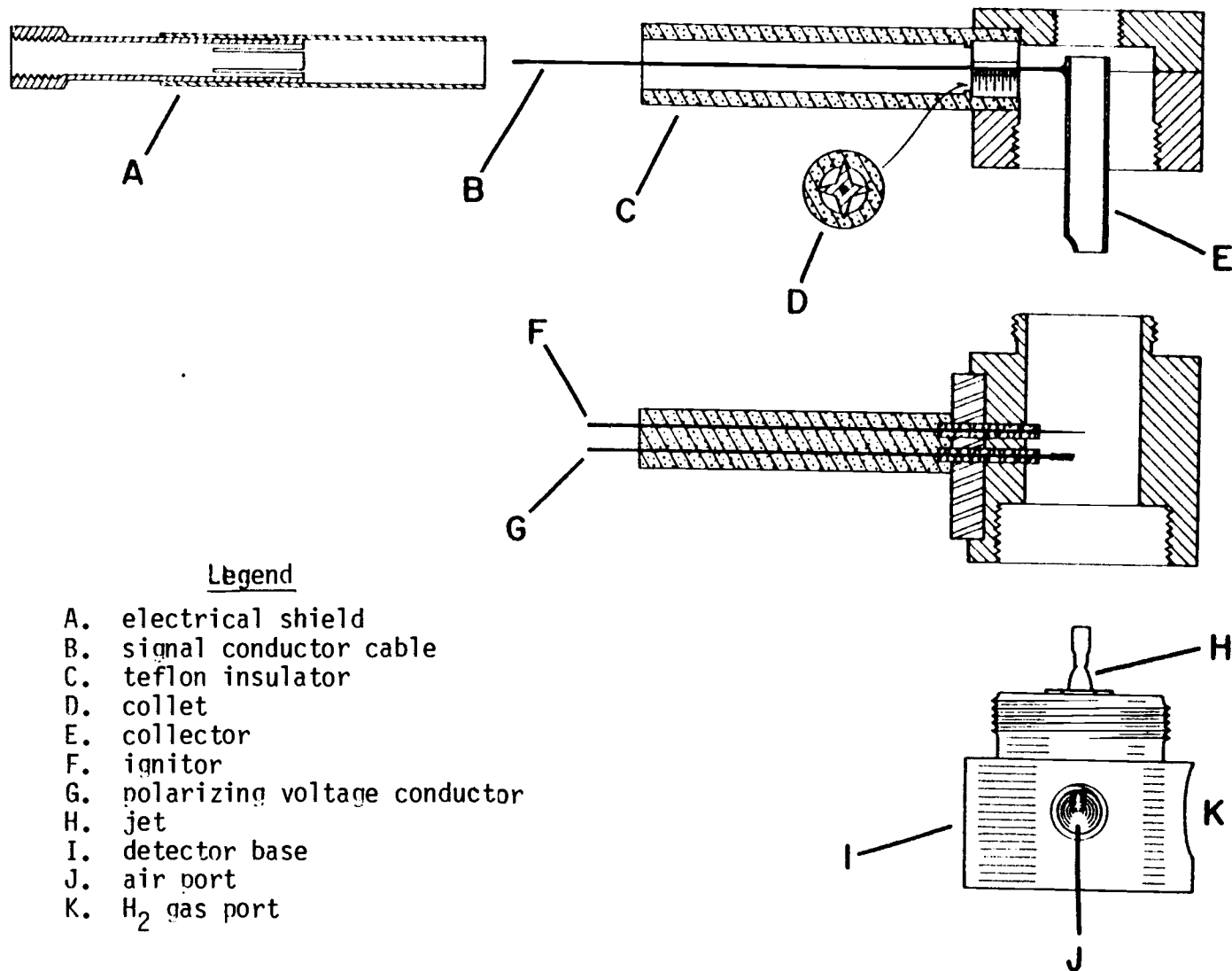
Fig. 4 flow diagram of gas chromatography system

- (a) helium inlet
- (b) needle valves
- (c) preheating column
- (d) injector
- (e) first reference column
- (f) first main column
- (g) thermal conductivity detector
- (h) differential pressure transducer
- (i) sampling valves
- (j) second main column
- (k) bypass column
- (l) stream splitter
- (m) flame ionization detector
- (n) exit valve from TCD
- (o) exit valve from FID
- (p) mercury barometer

they all had their detector jets mounted in such a way that the dead volume between the column and the flame was more than 100 microliters. For these reasons the FID designed by Dandeneau⁽¹⁶⁾ is used. The details of the flame ionization detector design are shown in Figure 4-6. The detector has many features. The collector-signal conductor assembly shown in the top part of Figure 4 is about 5 inches long when together and has air as the insulator between the shield and the signal conductor. The details of the detector base are shown in Figure 5. The internal diameter of the jet is 0.020 inches. The capillary tube (0.017 cm) coming from the splitter and carrying a fraction of the column effluent is clearly shown in Figure 6 to have penetrated most of the jet. This reduced the dead volume in the detector from just over a 100 μ l to less than 20 μ l with half of the dead volume being swept out by the inert gas (He) flow entering through the restrictor (C of Figure 5).

Splitter

The detail of a splitter at the end of the column is given in Figure 7. A 0.017 cm i.d. capillary tube connecting the FID jet and the column (extended 1.5 in. into the column) was found by Yang⁽⁶⁾ to be the best design in eliminating tailing of the peak due to end effect, back diffusion and the disturbance of the flow profile at the splitter.



Legend

- A. electrical shield
- B. signal conductor cable
- C. teflon insulator
- D. collet
- E. collector
- F. ignitor
- G. polarizing voltage conductor
- H. jet
- I. detector base
- J. air port
- K. H₂ gas port

Fig. 4 exploded view of flame ionization detector. Cross areas are stainless steel. Dotted areas are teflon.

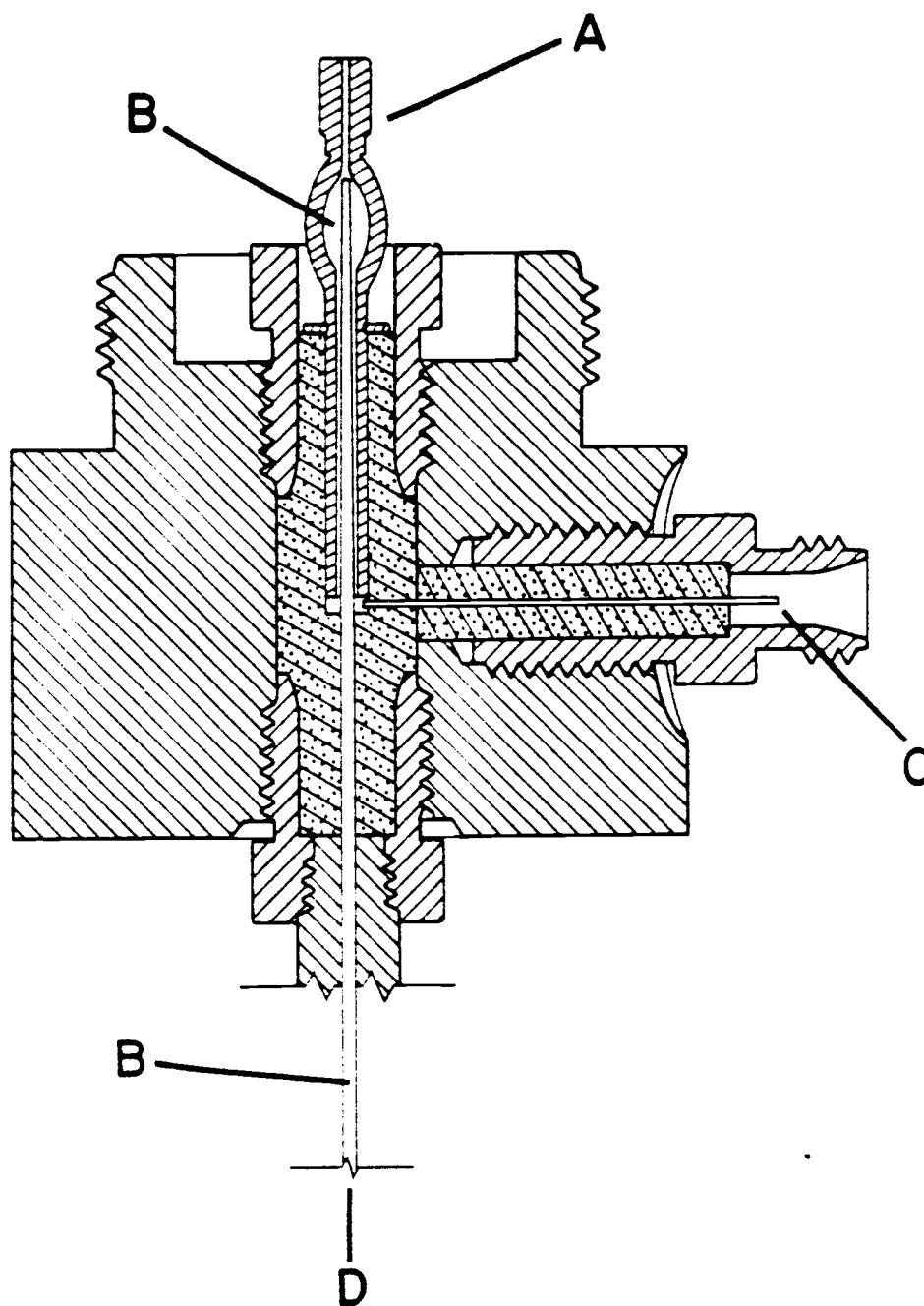


Fig. 5 detector base.

Cross hatched areas are stainless steel. Dotted areas are teflon. A. jet; B. splitter capillary; C. H₂ gas line restrictor; D. to splitter - column assembly.

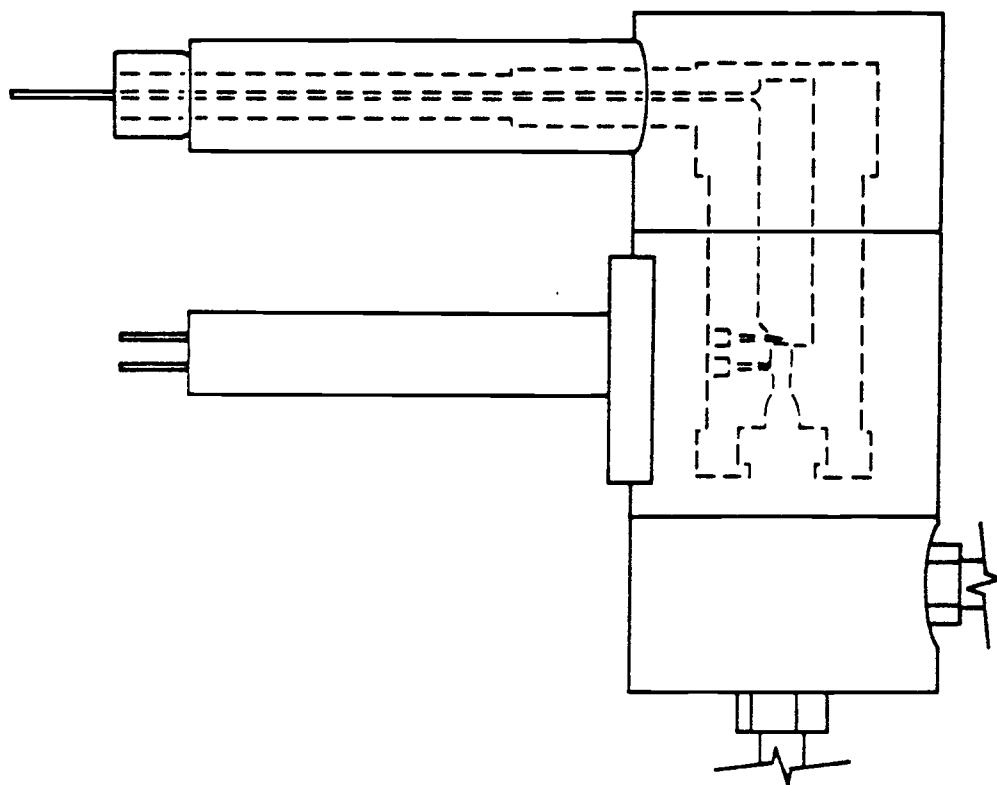


Fig. 6 assembled view of detector

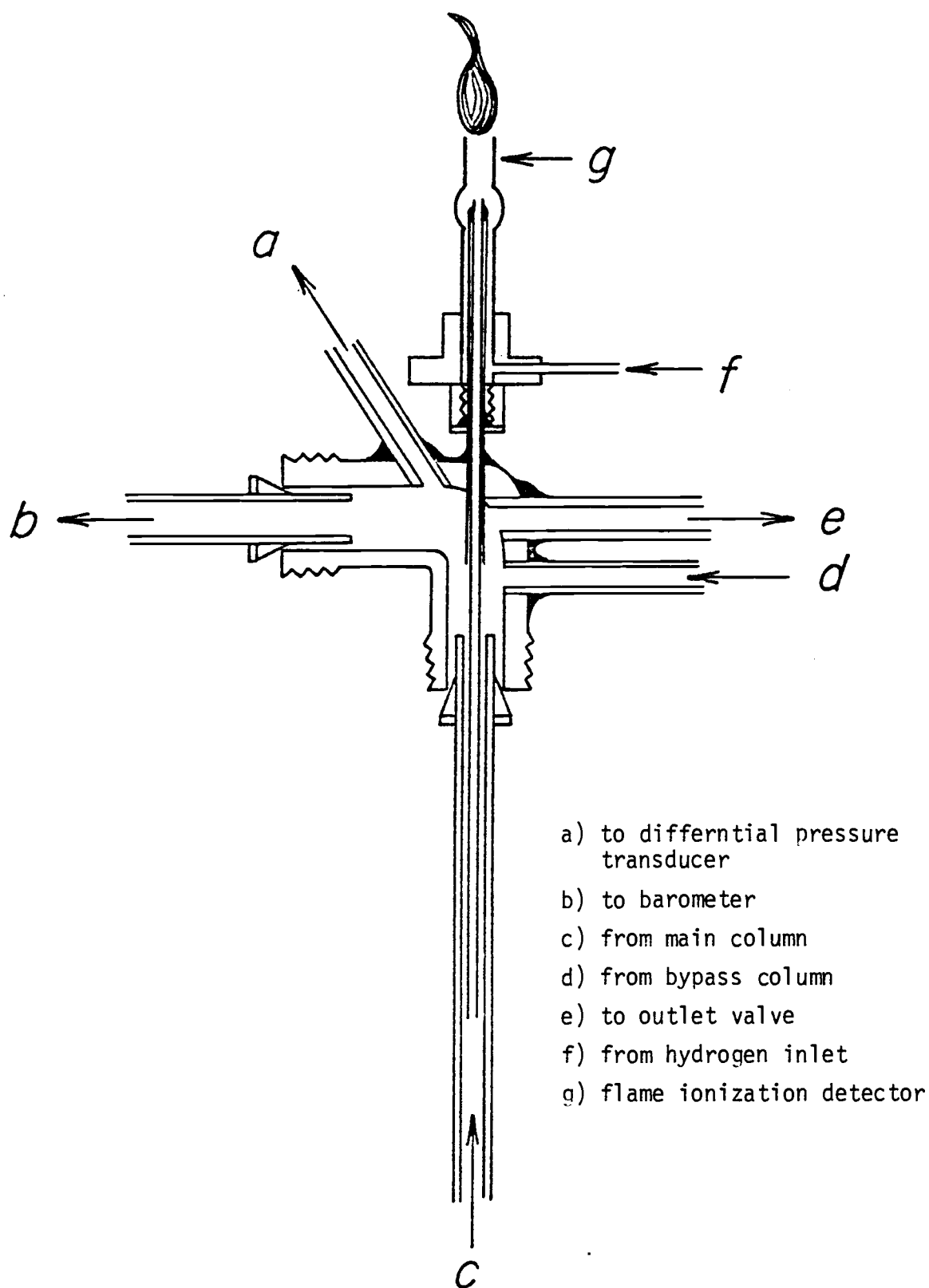


Fig. 7 stream splitter

Column

The preheating column c has a dimension of 45 ft x 0.25 in.o.d. x 0.120 in.i.d. copper. It serves the purpose of preheating the carrier gas and also serves as a buffer system for the stability of pressure and flow rate.

The first main column f has a dimension of 82 ft. x 1/16 in.o.d. x 1/32 in.i.d. stainless steel. It serves the purpose of eluting the sample and entering TCD for sampling the top part of the peak for the arrested elution.

The length and radius of the second main column j were measured by weighing the mercury contained within the void volume of the column and comparing against the weight of mercury inside a short column cut from the same delivery whose length can be precisely measured by using an engineering ruler. A 316 stainless steel column with an effective length of 304.8 cm was used in this study. The radius of the column was calculated by using the above data and the density data of mercury at that temperature (24°C). The value of the radius is 0.2184 cm. The curvature of both columns studied here was 10 cm.

Differential Pressure Transducer

The pressure gradient between the inlet and the outlet of the column was measured by using a 1.0 psi differential pressure transducer (Model KP15, Whittaker Corp., Hollywood, California) with a precision

of 0.1%. The pressure at the outlet of the column was measured by a mercury barometer.

Waterbath

Temperature was controlled by a Techne TE3 Quadrac Control waterbath. The temperature in the waterbath was measured by TC 100 thermometer (Electromedics, Inc., Englewood, Colorado).

Sampling Valve

A Model L-206-6 (Loenco, Inc., Altadena, California) valve was employed as the sampling valve. The valve has low dead volume between ports. How it is mounted in the chromatograph is shown in Figure 4.

B. Operation of the Apparatus

At first the sample used here was methane gas (c.p) with a minimum purity of 99.0%. Since the accuracy of our measurements was better than 1%, this is a lower purity than desirable. But fortunately the most likely impurity is hydrogen which is invisible to the flame ionization detector used and so has no effect on the result. If there were 1.0% of ethane present, our result would be $\frac{1}{4}\%$ low which is about the limit of our experimental reliability. Hence the 99.0% of purity of the methane is adequate. Then propane (99.99% purity) supplied by Matheson Gas Products was used. Helium gas (99.995% purity) was used as carrier gas.

Helium carrier gas supply was controlled at 10 psi gauge pressure at the regulator. The flow rate of the carrier gas stream was precisely controlled by one buffer and two needle valves located just in the front of the preconditioning column, and by a needle valve at the exit. The flow rate of the carrier stream was measured by computing the first moment of the elution peak.

0.20 ml of methane or 0.1 ml of propane was injected into the first main column. The thermal conductivity detector detected the elution peak of the sample. The top part of the peak is bypassed into the second main column. As the solute zone had migrated about half-way along the second main column, it was arrested for 5 minutes by pushing the second sampling valve to allow the carrier flow to enter into the bypass system in order to maintain constant pressure in the column. Finally the carrier gas was resumed by pulling the second sampling valve and the concentration profile of the eluted peak was detected by the FID system. The current source output from the FID was converted to voltage and amplified to the magnitude of about 1V, and collected directly on the computer interface. The program, EAGLEB, was called to transport the values in the computer interface to the Computer Center's CYBER 170/720. The operation of the interface is shown in Appendix A.

About 240 data points were collected for each elution peak. Time base was corrected and first moment was calculated by the statistical analysis program CODATA (Appendix B). BMDPAR, a derivative-free nonlinear regression, which was developed by UCLA, was then employed to compute the least squares fit D_{12}^* value. Two separate runs were conducted for each experimental condition. The control language for calling BMDPAR and the subroutine of the fit equation is shown in

Appendix C. A sample of the computer output for fitting concentration profile and obtaining D_{12}^* is shown in Appendix D.

Flow rates were in the range 3.06-3.68 cm/s and the temperature was in the range of $20-60 \pm 0.1^\circ\text{C}$. The pressure gradient across the column was 0.001 psi.

IV. Results and Discussion

Highly precise and accurate D_{12}^* values can be obtained only from a GC system which has a minimum contribution to the zone broadening due to its end effect, secondary flow effect, racetrack effect, turbulence, concentration effect, skewing or any other sources.

Direct calculation from Equation 5 had shown that the column utilized here should make no extra contribution to zone broadening due to the secondary flow effect under these experimental conditions and from Equation 6 about 0.006% contribution from the racetrack effect.

In addition, turbulence is not usually encountered in the open tubes for Reynolds numbers < 1800 ⁽¹⁷⁾. It was calculated that the linear velocity would have to be 143 cm/sec to get $Re = 30$ for these experiments with methane and propane in the 0.2184 cm i.d. open tube. Our velocity was no more than 3.7 cm/sec and therefore turbulence is not considered in this work. Grushka⁽¹⁸⁾ found that alkanes adsorbed on open tubular columns less than 0.54 cm i.d., regardless of how well the tubing was cleaned. This is noticeable for sample size below 0.1 micromole. With larger samples, broadening increased negligibly slowly. In this work, 0.8 micromole propane or methane was used. So, the concentration effect is negligible. Summarily, the effect of these extra zone broadening factors can be presumed to be negligible. If they were not, their effect could easily be observed from the standard error of the fitted parameter D_{12}^* , since Yang and Hawkes⁽⁶⁾ has shown that they mainly affect the tails of the peak.

D_{12}^* values obtained from methane are tabulated in Table 1. It gave an average D_{12}^* value of 0.6431 cm²/s and a standard deviation of

Table I. Binary Molecular Diffusion Coefficient ($\text{CH}_4\text{-He}$)

Velocity cm/S	Arrested Time, S	D_{12}^* , cm^2/s from least squares fit	Standard error of D_{12}^* from least squares fit
3.175	300	0.6448	2.0×10^{-3}
3.129	300	0.6413	1.7×10^{-3}

Average 0.6431

Standard Deviation 0.0025

0.0025 absolute. The value obtained by interpolating between Yang's values at 15° and 20°C is 0.6446 cm²/sec which is in good agreement, indicating that our modified apparatus is satisfactory. Table II shows the average values of the diffusion coefficients of the propane-helium gas pair obtained at 21.3, 30.3, 40.1, 51.0 and 61.3°C. The precision of the measurements was in the range of 0.27 to 0.34%. Further, the indication of the precision and the reliability of the measurements is shown by the least-squares plot of $\log D_{12}^*$ vs $\log T$ (T is absolute temperature) in Figure 8. The correlation coefficient is 0.9976. The slope of this least-squares straight line give a 3.0805 temperature power dependence of D_{12}^* . The intercept is -8.1277. Accordingly, we offer the equation

$$\log D_{12}^* = -8.1277 + 3.0805 \log T \quad (19)$$

Table III shows the comparison of experimental and calculated values.

Table II. Binary Molecular Diffusion Coefficient (C_3H_8 - He)

Velocity cm/S	Arrested Time, S	Temp °C	D_{12}^* cm ² /S from least squares, fit	Standard error of D_{12}^* from least squares fit
2.938	300	21.3	0.3005	1.0×10^{-3}
3.060	300	30.3	0.3292	1.0×10^{-3}
3.192	300	40.1	0.3601	1.0×10^{-3}
3.461	300	51.0	0.4132	1.1×10^{-3}
3.678	300	60.3	0.4365	1.5×10^{-3}

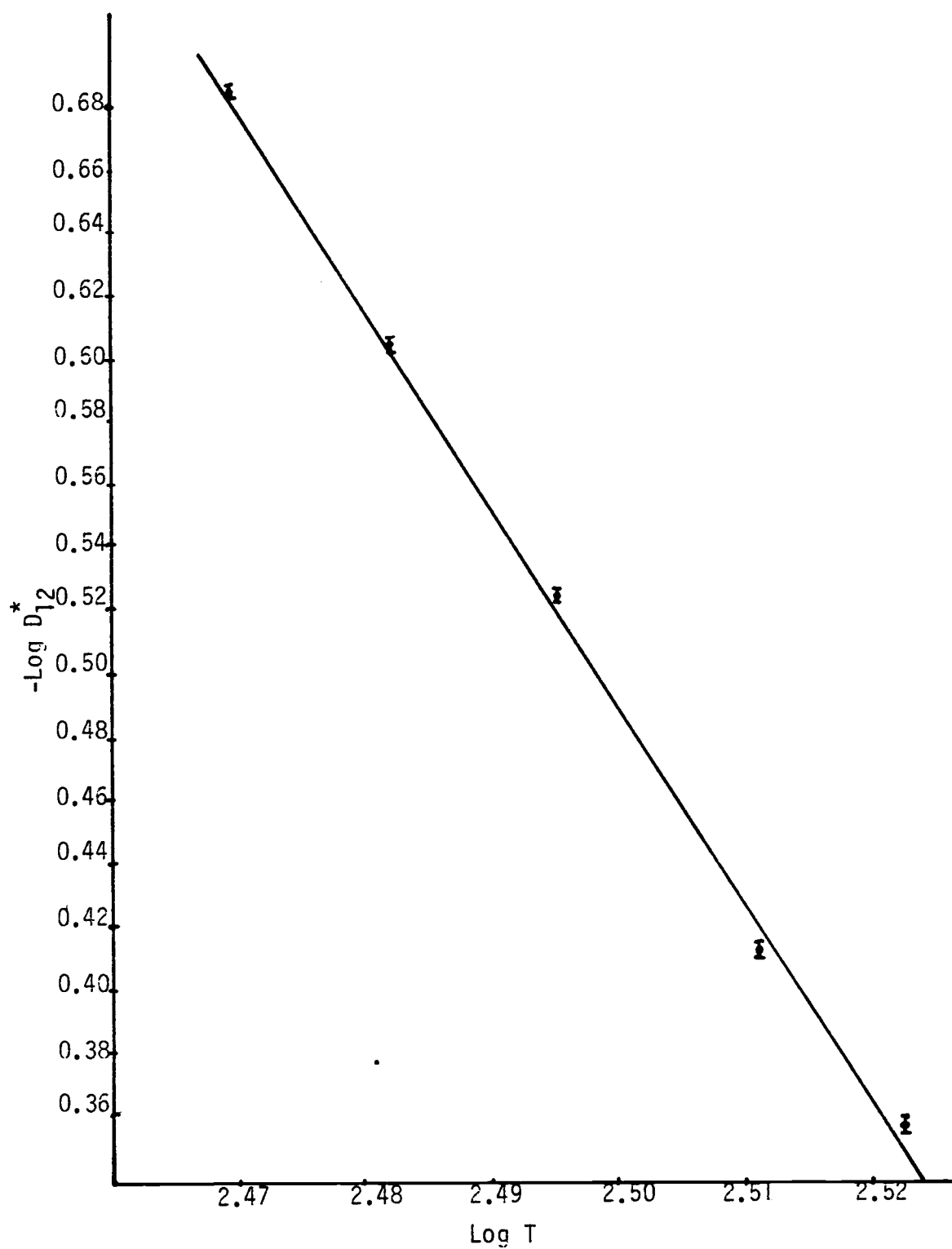


Fig. 8 $-\text{Log } D_{12}^*$ vs. $\text{Log } T$ for the C_3H_8 -He system

Table III. Comparison of Experimental and Calculated Diffusion

Coefficients (C_3H_8 - He)			
Temp °C	D_{12}^* cm ² /s (exptl)	D_{12}^* cm ² /s (From eq 19)	Difference (calcd-exptl)
21.3	0.3005 ± 0.0010	0.3002	-0.0003
30.3	0.3292 ± 0.0010	0.3295	+0.0003
40.1	0.3601 ± 0.0010	0.3633	+0.0022
51.0	0.4104 ± 0.0011	0.4036	-0.0068
60.3	0.4365 ± 0.0015	0.4403	+0.0038

V. Conclusions

The apparatus discussed here has been successful in rapidly obtaining experimental gaseous diffusion data. The object of this research has been the exploration of the applicability. Although it is adequate for many purposes, significant improvements are possible which should reduce time. It would be useful for the compilation of extensive diffusion data. The apparatus could be operated with automatic injection and sampling system. Therefore the sampling measurement and calculation can be operated automatically and continuously.

Bibliography

1. J.C. Giddings and S.L. Seager, J. Chem. Phys., 33, 1579 (1960).
2. J.C. Giddings and S.L. Seager, J. Chem. Phys., 35, 2242 (1961).
3. J.C. Giddings and S.L. Seager, Ind. Eng. Chem., Fundam., 1, 227 (1962).
4. J.H. Knox and L. McLaren, Anal. Chem., 36, 1477 (1964).
5. Sir Geoffrey Taylor, Proc. Roy. Soc., (London) A219, 186 (1953).
6. Frank Yang, Stephen Hawkes, and F.T. Lindstrom, J. A. Chem. Soc., 98, 5101 (1976).
7. C.M. White, Proc. Roy. Soc. London, Ser. A., 123, 645 (1929).
8. J.C. Gidding, J. Chromatogr., 1, 520 (1960).
9. Frank J. Yang and Stephen J. Hawkes, J. Chem. Eng. Data., 24, 354 (1979).
10. A.T. James and A.J.P. Martin, Biochem. J., 50, 679 (1952).
11. J.C. Giddings, S.L. Seager, L.R. Stucki and G.H. Steward, Anal. Chem., 32, 867 (1960).
12. P.E. Porter, A.I.M. Keulemans and F.H. Stross, J. Am. Chem. Soc., 78, 2999 (1956).
13. Ott Grubner, Statistical Moments Theory of Gas-solid Chromatography: Diffusion-Controlled Kinetics. In, "Advances in Chromatography," Vol. 6, ed. J.C. Giddings and R.A. Keller, pub. Marcel Dekker, 1965, p. 173.
14. Richard Dick and C. Harold Hartmann, "Critical Evaluation of the Response Characteristics of the Hydrogen Flame Detector," Varian Aerograph, 1966.
15. E.H. Piepmeier, "Chemistry and Instruments," Chemistry Department, Oregon State University.
16. Raymond Dale Dandeneau, "Fast Gas Chromatography," Ph.D. Thesis, Chemistry Department, Oregon State University, 1978.
17. F. Doue and G. Guiochon, Separation Sci., 5, 197 (1970).
18. B.E. Bowen and S.P. Cram, J. Chromatogr. Sci., 12, 579 (1974).

Appendix A

The Operation of Computer Interface

I. Operation of Interface

1. Turn on interface and teletype
2. Call Computer Center, extension 2033 and ask to have this computer channel (Patch 180 to 110 Baud) plugged in.
3. Now that we are logged on, make these initial settings of the registers on the interface (See II).

Time Base	XXX
K	XXX
L	XXX
M	XXX
N	XXX
TS	XXX
ID	XXX

4. Push the reset button.
5. Push the start button.
6. Now the interface begins to collect data.

II. Setting of the Registers

Time Base

The setting of this switch register determines the time (seconds) that should elapse between each data point. For example, if you want to sample the data once every 0.1, 0.02 or 0.005 seconds, you would set the switches to 1×10^{-1} , 2×10^{-2} or 5×10^{-3} .

K

This register sets a delay between the time that the interface receives the Start Data signal and the first actual sample of data. The amount of delay is equal to the product of the K and Time Base registers. For example, the Time Base was set to 1×10^{-1} and the K was set 50×10^1 or 08×10^0 .

$$(50 \times 10^1) \times (1 \times 10^{-1}) = 50 \text{ seconds}$$

or

$$(8 \times 10^0) \times (1 \times 10^{-1}) = 0.8 \text{ seconds}$$

it was 50 or 0.8 seconds before the acquiring light comes on.

L

The register determines a number of samples to be taken. If the L register was set to 35×10^2 or 09×10^0 , then 3500 or 9 samples would be taken by the interface at a rate determined by the Time Base.

M

This register sets another delay and is determined in exactly the same way as was K. This delay is between two strings of data.

N

This register determines the final number of samples to be taken.

Note: No one register can be set to zero. Also, remember to push the Reset button after changing any register and before starting the data.

The Program of Dumping Data to the Computer

After the interface has collected the data, type the following on the teletype.

/GET, EAGLE B

/EAGLE B

TB: XXX

K: XXX

L: XXX

M: XXX

N: XXX

TS: XXX

ID: XXX

-START-

(ASCII code printed)

/SAVE, TAPE1 = file name

/BYE.

Note: (i) XXX means value which needs to be input. If K is set 30×10^2 or 05×10^0 , 302 or 50 is input from teletype as K appears. The other inputs are in the same way. When entering TB, ignore the negative sign. E.g. 3×10^{-3} is entered as 33.

(ii) TS is the arrested time. If the arrested time was 300 seconds and Time Base was 0.1 seconds the value

$$\frac{300}{0.1} = 3000 = 30 \times 10^2$$

302 was input from teletype as TS appeared.

(iii) ID is the identification number for your records only.

It is input in the same way as the other registers.

- (iv) The output Format is (f6.0, F8.3). F6.0 is for the signal and F8.3 is for time spent mobile.
- (v) As -START- appears, push the Dump Enable button and then the Dump button.

Appendix B

Fortran Program for the Correction of the Time Base.
Output Signal and the Calculation of Sample Peak Statistics.

.


```

PROGRAM CODATA (data filename, TAPE 5 = date filename, TAPE 6).
DIMENSION CONC (240), TIME (240), FCONC (240)
TCD = XXX
C1 = 0.0
C2 = 0.0
C3 = 0.0
CT = 0.0
10 DO 40 I = 1,240
   READ (5,20)CONC(I),TIME(I)
20   FORMAT (F6.0,F8.3)
   TIME(I) = TIME(I)-TCD
   CONC(I)=CONC(I)**1.01
   CT=CT + TIME(I)*CONC(I)
   C1 = C1+CONC(I)
   WRITE(6,30)CONC(I),TIME(I)
30   FORMAT (F6.0,F8.3)
40   CONTINUE
   TMEAN=CT/C1
   DO 50 I=1,240
   FCONC(I)=CONC(I)/C1
50   CONTINUE
   DO 60 I=1,240
   C2=C2+(TIME(I)-TMEAN)**2*FCONC(I)
   C3=C3+(TIME(I)-TMEAN)**3*FCONC(I)
60   CONTINUE
   G=C3/C2**1.5
   WRITE(6.70)TMEAN,G
70   FORMAT(2F8.3)
   STOP
   END

```

Note: (i) 240 is the number of data.

(ii) TCD is the mean time of the peak from TCD. It needs to be input before the program is run.

Appendix C

Control Language for Calling BMDP-AR and the
Subroutine of the Fit Equation

(I) The Subroutine of the Fit Equation

```

SUBROUTINE FUN (F,P,X,N,KASE,NVAR,NPAR,IPASS,XLOSS)
DIMENSION P(NPAR),X(NVAR)

AL = XXXX      (AL is length of the column)
AP = XXXX      (AP is pressure)
AR = XXXX      (AR is radius of the column)
TS = XXX       (TS is the arrested time)
AV = XXX       (AV is the velocity of the carrier gas)

B=AL*(P(1)/AP + AR**2*AV**2*AP/(48.0*P(1)))+AV*TS*P(1)/AP
C=((P(1)/AP+AR**2*AV**2*AP/(48.0*P(1)))*X(2)+TS*P(1)/AP)
D=(-0.25)*(AL-AV*X(2))**2/C
F=P(2)*B/(3.54491*C**1.5)*EXP(D)

RETURN

END

```

(II) Control Language For Calling BMDP-AR

```

/PROBLEM      TITLE IS 'DIFFUSION OF PROPANE'.
/INPUT        VARIABLES=2. UNIT=12.FORMAT IS'(F 6.0,F8.3)'.
/VARIABLE     NAMES ARE CONC. TIME.
/REGRESS      DEPENDENT IS CONC. PARAMETER ARE 2.
/PARAMETER    INITIAL ARE XXXX.XXXXX.
/END

```

Note: Before this program is run, two guessed values for diffusion coefficient and initial concentration need to be input.

Note: The above program must be recorded in a file with a name, referred to later as the control language file name.

(III) Procedure of Running BMDP-AR

/GET, data filename (see Appendix B)

/GET, control language file name (see Appendix C.II)

/GET, subroutine filename (i.e. FUN, see Appendix C.I)

/-BMDP 81,,BMDPAR

/ATTACH,FIN4/UN=LIBRARY

/FIN4 (I=subroutine filename, L=0)

/BMDPAR, I=control language filename, D=data filename, B

(About 2 minutes will elapse before data is printed out.)

Appendix D

A Sample of the Computer Output for Fitting
Fitting Concentration Profile and Obtaining
 D_{12}^*

PAGE 1

BMDPAR--DERIVATIVE-FREE NONLINEAR REGRESSION
 DEPARTMENT OF BIOMATHEMATICS
 UNIVERSITY OF CALIFORNIA, LOS ANGELES, CA 90024
 (213) 825-5940 TWX UCLA LSA
 PROGRAM REVISED JUNE 1981
 MANUAL REVISED -- 1981
 COPYRIGHT (C) 1981 REGENTS OF UNIVERSITY OF CALIFORNIA
 EXECUTED ON 83/04/11 AT 21.58.20.

TO SEE REMARKS AND A SUMMARY OF NEW FEATURES FOR
 THIS PROGRAM, STATE NEWS. IN THE PRINT PARAGRAPH.
 THIS VERSION OF BMDP HAS BEEN CONVERTED FOR USE ON
 CDC 6000 AND CYBER SERIES COMPUTERS BY
 BMDP PROJECT, VOGELBACK COMPUTING CENTER
 NORTHWESTERN UNIVERSITY
 2129 SHERIDAN ROAD
 EVANSTON, ILLINOIS 60201

PROGRAM CONTROL INFORMATION

```
/PROBLEM      TITLE IS 'DIFFUSION OF PROPANE'.
/INPUT        VARIABLES=2.UNIT=12.FORMAT IS '(F6.0,F8.3)'.
/VARIABLE     NAMES ARE CONC,TIME.
/REGRESS      DEPENDENT IS CONC.PARAMETER ARE 2.
/PARAMETER    INITIAL ARE .400,10000.0.
/END
```

BMDP UNIT NO. 12 SPECIFIED IN THE INPUT PARAGRAPH
 WILL REFER TO LOCAL FILE NAME CDAT21 FOR THIS PROBLEM.

PROBLEM TITLE IS
 DIFFUSION OF PROPANE

```
NUMBER OF VARIABLES TO READ IN. . . . . 2
NUMBER OF VARIABLES ADDED BY TRANSFORMATIONS. . . . . 0
TOTAL NUMBER OF VARIABLES . . . . . 2
NUMBER OF CASES TO READ IN. . . . . TO END
CASE LABELING VARIABLES . . . . .
MISSING VALUES CHECKED BEFORE OR AFTER TRANS. . . . . NEITHER
BLANKS ARE. . . . . MISSING
INPUT UNIT NUMBER . . . . . 12
REWIND INPUT UNIT PRIOR TO READING. . . . . YES
NUMBER OF WORDS OF DYNAMIC STORAGE. . . . . 9996
NUMBER OF CASES DESCRIBED BY INPUT FORMAT . . . . . 1
```

VARIABLES TO BE USED
 1 CONC 2 TIME

PAGE 2 DIFFUSION OF PROPANE

INPUT FORMAT IS
(F6.0,F8.3)

MAXIMUM LENGTH DATA RECORD IS 14 CHARACTERS.

I N P U T V A R I A B L E S						
VARIABLE		RECORD	COLUMNS		FIELD	TYPE
INDEX	NAME	NO.	BEGIN	END	WIDTH	
-----		----	-----	-----	-----	----
1	CONC	1	1	6	6	F

VARIABLE		RECORD	COLUMNS		FIELD	TYPE
INDEX	NAME	NO.	BEGIN	END	WIDTH	
-----		----	-----	-----	-----	----
2	TIME	1	7	14	8.3	F

PAGE 3 DIFFUSION OF PROPANE

REGRESSION TITLE
DIFFUSION OF PROPANE

REGRESSION NUMBER	0
DEPENDENT VARIABLE	CONC
WEIGHTING VARIABLE	
NUMBER OF PARAMETERS	2
NUMBER OF CONSTRAINTS	0
TOLERANCE FOR PIVOTING	1.0E-08
TOLERANCE FOR CONVERGENCE	1.0E-05
MAXIMUM NUMBER OF ITERATIONS	50
MAXIMUM NUMBER OF INCREMENT HALVINGS	5

PARAMETERS TO BE ESTIMATED

	1 P1	2 P2
MINIMUM	-.212676E+38	-.212676E+38
MAXIMUM	.212676E+38	.212676E+38
INITIAL	.400000	10000.000000

USING THE ABOVE SPECIFICATIONS THIS PROGRAM COULD USE UP TO 753 CASES.

BASED ON INPUT FORMAT SUPPLIED 1 RECORDS READ PER CASE.

++ DATA ERROR(S) IN CASE NO. 221		++ VARIABLE RECORD COLUMNS		++ CONTENTS OF FIELD		++ ILLEGAL		++ OCTAL	
++ INDEX	++ NAME	++ NO.	++ BEGIN	++ END	++ IN ERROR	++ CHARACTER	++	++	++
++	2 TIME	1	7	14	"46	" "			555555
++ RECORD CONTAINING ERROR(S)									

103.746
S

NUMBER OF CASES READ	221
CASES WITH DATA MISSING OR BEYOND LIMITS . . .	1
REMAINING NUMBER OF CASES	220

VARIABLE NO. NAME	MEAN	STANDARD DEVIATION	MINIMUM	MAXIMUM
1 CONC	248.663636	285.210465	-3.000000	822.000000
2 TIME	97.413000	12.730541	75.513000	119.313000

ITER. INCR.	RESIDUAL SUM	PARAMETERS
NO. HALV.	OF SQUARES	1 P1 2 P2

USER ROUTINE FUN LOADED FROM FILE LGO AT ADDRESS 077416B.

0	0	1262170.737888	.440000	10000.000000
0	0	893972.977793	.400000	10000.000000
0	0	379093.110030	.400000	11000.000000
1	0	79448.028355	.265302	10823.652308
2	0	11466.528117	.308548	10934.004359

3	2	11211.853231	.308408	10953.420081
4	0	8891.574687	.300568	10889.475862
5	0	8889.533847	.300631	10893.015170
6	2	8889.527836	.300630	10893.091429
7	0	8888.741960	.300490	10891.933617
8	0	8888.741556	.300489	10891.919494
9	5	8888.741596	.300489	10891.907092
10	0	8288.741259	.300486	10891.897951
11	0	8888.741269	.300486	10891.897311
12	3	8888.741269	.300486	10891.897059

PAGE 4 DIFFUSION OF PROPANE

THE RESIDUAL SUM OF SQUARES (= 8888.74) WAS SMALLEST WITH

1 P1	2 P2
.300486	10891.9

ESTIMATE OF ASYMPTOTIC CORRELATION MATRIX

	P1		P2	
		1		2
P1	1	1.0000		
P2	2	.5779	1.0000	

THE ESTIMATED MEAN SQUARE ERROR IS 40.77

ESTIMATES OF ASYMPTOTIC STANDARD DEVIATIONS OF PARAMETER ESTIMATES WITH 218 DEGREE

1 P1	2 P2
1.019567E-03	15.2056

PAGE 5 DIFFUSION OF PROPANE

CASE NO. NAME	RESIDUAL	OBSERVED 1 CONC	PREDICTED 1 CONC	STD. DEV. PREDICTED	2 TIME
1	13.999764	14.000000	.000236	.000011	75.5130
2	-3.000295	-3.000000	.000295	.000014	75.7130
3	-3.000367	-3.000000	.000367	.000017	75.9130
4	-2.000457	-2.000000	.000457	.000021	76.1130
5	-2.000567	-2.000000	.000567	.000026	76.3130
6	-3.000703	-3.000000	.000703	.000032	76.5130
7	-2.000870	-2.000000	.000870	.000039	76.7130
8	-2.001075	-2.000000	.001075	.000047	76.9130
9	-2.001326	-2.000000	.001326	.000057	77.1130
10	-1.001632	-1.000000	.001632	.000069	77.3130
11	-.002005	0.000000	.002005	.000083	77.5130
12	-2.002460	-2.000000	.002460	.000101	77.7130
13	-1.003012	-1.000000	.003012	.000121	77.9130
14	-2.003682	-2.000000	.003682	.000146	78.1130
15	-2.004493	-2.000000	.004493	.000175	78.3130
16	-2.005473	-2.000000	.005473	.000210	78.5130
17	-1.006655	-1.000000	.006655	.000251	78.7130
18	-1.008079	-1.000000	.008079	.000299	78.9130
19	-1.009791	-1.000000	.009791	.000356	79.1130
20	-1.011845	-1.000000	.011845	.000424	79.3130
21	-1.014304	-1.000000	.014304	.000503	79.5130
22	-1.017245	-1.000000	.017245	.000596	79.7130
23	-1.020755	-1.000000	.020755	.000704	79.9130
24	-2.024937	-2.000000	.024937	.000831	80.1130
25	-2.029910	-2.000000	.029910	.000979	80.3130
26	-2.035813	-2.000000	.035813	.001151	80.5130
27	-2.042809	-2.000000	.042809	.001351	80.7130
28	-3.051083	-3.000000	.051083	.001582	80.9130
29	-2.060854	-2.000000	.060854	.001850	81.1130
30	-3.072372	-3.000000	.072372	.002159	81.3130
31	-2.085923	-2.000000	.085923	.002515	81.5130
32	-2.101839	-2.000000	.101839	.002924	81.7130
33	-2.120500	-2.000000	.120500	.003394	81.9130
34	-2.142341	-2.000000	.142341	.003931	82.1130
35	-2.167857	-2.000000	.167857	.004545	82.3130
36	-1.197616	-1.000000	.197616	.005245	82.5130
37	-1.232261	-1.000000	.232261	.006042	82.7130
38	-1.272524	-1.000000	.272524	.006946	82.9130
39	-.319233	0.000000	.319233	.007971	83.1130
40	-1.373323	-1.000000	.373323	.009130	83.3130
41	-.435853	0.000000	.435853	.010438	83.5130
42	-.508012	0.000000	.508012	.011912	83.7130
43	1.408866	2.000000	.591134	.013567	83.9130
44	-.686720	0.000000	.686720	.015424	84.1130
45	1.203557	2.000000	.796443	.017502	84.3130
46	.077825	1.000000	.922175	.019822	84.5130
47	1.934004	3.000000	1.065996	.022408	84.7130
48	.769778	2.000000	1.230222	.025283	84.9130
49	2.582581	4.000000	1.417419	.028473	85.1130
50	1.369576	3.000000	1.630424	.032005	85.3130
51	3.127628	5.000000	1.872372	.035907	85.5130
52	2.853287	5.000000	2.146713	.040208	85.7130
53	2.542763	5.000000	2.457237	.044939	85.9130
54	3.191899	6.000000	2.808101	.050130	86.1130
55	2.796150	6.000000	3.203850	.055813	86.3130
56	4.350556	8.000000	3.649444	.062022	86.5130
57	3.849722	8.000000	4.150278	.068789	86.7130

58	4.287785	9.000000	4.712215	.076147	86.9130
59	4.658399	10.000000	5.341601	.084130	87.1130
60	3.954707	10.000000	6.045293	.092769	87.3130
61	4.169317	11.000000	6.830683	.102096	87.5130
62	5.294286	13.000000	7.705714	.112142	87.7130
63	5.321099	14.000000	8.678901	.122934	87.9130
64	5.240651	15.000000	9.759349	.134501	88.1130
65	6.043233	17.000000	10.956767	.146865	88.3130
66	6.718524	19.000000	12.281476	.160048	88.5130
67	6.255579	20.000000	13.744421	.174066	88.7130
68	5.642830	21.000000	15.357170	.188935	88.9130
69	6.868082	24.000000	17.131918	.204661	89.1130
70	6.918524	26.000000	19.081476	.221248	89.3130
71	6.780740	28.000000	21.219260	.238694	89.5130
72	7.440724	31.000000	23.559276	.256989	89.7130
73	7.883905	34.000000	26.116095	.276118	89.9130
74	8.095182	37.000000	28.904818	.296058	90.1130
75	9.058957	41.000000	31.941043	.316777	90.3130
76	8.759188	44.000000	35.240812	.338236	90.5130
77	8.179439	47.000000	38.820561	.360387	90.7130
78	9.302944	52.000000	42.697056	.383172	90.9130
79	8.112683	55.000000	46.887317	.406524	91.1130
80	9.591458	61.000000	51.408542	.430368	91.3130
81	9.721987	66.000000	56.278013	.454616	91.5130
82	9.487001	71.000000	61.512999	.479176	91.7130
83	8.869353	76.000000	67.130647	.503940	91.9130
84	8.852134	82.000000	73.147866	.528797	92.1130
85	8.418799	88.000000	79.581201	.553622	92.3130
86	9.553300	96.000000	86.446700	.578287	92.5130
87	8.240227	102.000000	93.759773	.602652	92.7130
88	8.464952	110.000000	101.535048	.626573	92.9130
89	7.213787	117.000000	109.786213	.649900	93.1130
90	7.474140	126.000000	118.525860	.672480	93.3130
91	6.234674	134.000000	127.765326	.694156	93.5130
92	5.485479	143.000000	137.514521	.714768	93.7130
93	5.218228	153.000000	147.781772	.734160	93.9130
94	3.426354	162.000000	158.573646	.752175	94.1130
95	3.105207	173.000000	169.894793	.768664	94.3130
96	1.252217	183.000000	181.747783	.783483	94.5130
97	-.132947	194.000000	194.132947	.796496	94.7130
98	-2.048227	205.000000	207.048227	.807583	94.9130
99	-2.489037	218.000000	220.489037	.816634	95.1130
100	-5.448129	229.000000	234.448129	.823562	95.3130
101	-3.915474	245.000000	248.915474	.828297	95.5130
102	-5.878153	259.000000	263.878153	.830797	95.7130
103	-8.320273	271.000000	279.320273	.831046	95.9130
104	-9.222884	286.000000	295.222884	.829064	96.1130
105	-10.563932	301.000000	311.563932	.824904	96.3130
106	-11.318222	317.000000	328.318222	.815662	96.5130
107	-12.457404	333.000000	345.457404	.810481	96.7130
108	-12.949982	350.000000	362.949982	.800553	96.9130
109	-13.761351	367.000000	380.761351	.789125	97.1130
110	-12.353853	386.000000	398.853853	.776505	97.3130
111	-13.186859	404.000000	417.186859	.763064	97.5130
112	-13.716882	422.000000	435.716882	.749236	97.7130
113	-13.397708	441.000000	454.397708	.735518	97.9130
114	-12.180557	461.000000	473.180557	.722467	98.1130
115	-12.014273	480.000000	492.014273	.710681	98.3130
116	-10.845526	500.000000	510.845526	.700788	98.5130
117	-10.619054	519.000000	529.619054	.693412	98.7130
118	-9.277912	539.000000	548.277912	.689138	98.9130
119	-7.763754	559.000000	566.763754	.688467	99.1130
120	-7.017125	578.000000	585.017125	.691779	99.3130

121	-5.977774	597.000000	602.977774	.699294	99.5130
122	-4.584985	616.000000	620.584985	.711057	99.7130
123	-3.777913	634.000000	637.777913	.726926	99.9130
124	-2.495934	652.000000	654.495934	.746599	100.1130
125	-.679005	670.000000	670.679005	.769632	100.3130
126	-.268019	686.000000	686.268019	.795485	100.5130
127	.794828	702.000000	701.205172	.823552	100.7130
128	1.565685	717.000000	715.434315	.853199	100.9130
129	3.098685	732.000000	728.901315	.883784	101.1130
130	3.445603	745.000000	741.554397	.914683	101.3130
131	4.655522	758.000000	753.344478	.945303	101.5130
132	4.774517	769.000000	764.225483	.975085	101.7130
133	6.845346	781.000000	774.154654	1.003519	101.9130
134	6.907176	790.000000	783.092824	1.030139	102.1130
135	6.995320	798.000000	791.004680	1.054530	102.3130
136	7.141007	805.000000	797.858993	1.076327	102.5130
137	7.371174	811.000000	803.628826	1.095214	102.7130
138	7.708291	816.000000	808.291709	1.110929	102.9130
139	8.170216	820.000000	811.829784	1.123256	103.1130
140	6.770080	821.000000	814.229920	1.132032	103.3130
141	6.516208	822.000000	815.483792	1.137144	103.5130
142	6.412077	822.000000	815.587923	1.138528	103.7130
143	6.456298	821.000000	814.543702	1.136169	103.9130
144	5.642642	818.000000	812.357358	1.130103	104.1130
145	5.960098	815.000000	809.039902	1.120413	104.3130
146	5.392958	810.000000	804.607042	1.107229	104.5130
147	5.920945	805.000000	799.079055	1.090731	104.7130
148	5.519361	798.000000	792.480639	1.071144	104.9130
149	4.159272	789.000000	784.840728	1.048738	105.1130
150	4.807714	781.000000	776.192286	1.022832	105.3130
151	3.427934	770.000000	766.572066	.996784	105.5130
152	1.979641	758.000000	756.020359	.967999	105.7130
153	.419291	745.000000	744.580709	.937923	105.9130
154	.700377	733.000000	732.299623	.907043	106.1130
155	.773746	720.000000	719.226254	.875877	106.3130
156	-.412082	705.000000	705.412082	.844975	106.5130
157	-.910579	690.000000	690.910579	.814916	106.7130
158	-1.776868	674.000000	675.776868	.786281	106.9130
159	-2.067385	658.000000	660.067385	.759651	107.1130
160	-2.839535	641.000000	643.839535	.735579	107.3130
161	-4.151349	623.000000	627.151349	.714561	107.5130
162	-4.061151	606.000000	610.061151	.697013	107.7130
163	-3.627231	589.000000	592.627231	.683233	107.9130
164	-3.907524	571.000000	574.907524	.673379	108.1130
165	-5.959312	551.000000	556.959312	.667455	108.3130
166	-5.838928	533.000000	538.838928	.665301	108.5130
167	-5.601482	515.000000	520.601482	.666615	108.7130
168	-5.300608	497.000000	502.300608	.670978	108.9130
169	-5.988229	478.000000	483.988229	.677885	109.1130
170	-5.714336	460.000000	465.714336	.686784	109.3130
171	-5.526797	442.000000	447.526797	.697115	109.5130
172	-5.471187	424.000000	429.471187	.708326	109.7130
173	-5.590633	406.000000	411.590633	.719906	109.9130
174	-4.925695	389.000000	393.925695	.731389	110.1130
175	-3.514257	373.000000	376.514257	.742365	110.3130
176	-3.391449	356.000000	359.391449	.752482	110.5130
177	-2.589587	340.000000	342.589587	.761444	110.7130
178	-2.138140	324.000000	326.138140	.769011	110.9130
179	-2.063707	308.000000	310.063707	.774991	111.1130
180	-1.390031	293.000000	294.390031	.779241	111.3130
181	-.138011	279.000000	279.138011	.781658	111.5130
182	-.325752	264.000000	264.325752	.782180	111.7130
183	1.031384	251.000000	249.968616	.780774	111.9130

184	.920705	237.000000	236.079295	.777440	112.1130
185	2.332099	225.000000	222.667901	.772204	112.3130
186	3.257944	213.000000	209.742056	.765111	112.5130
187	3.692995	201.000000	197.307005	.756228	112.7130
188	4.634266	190.000000	185.365734	.745639	112.9130
189	6.080909	180.000000	173.919091	.733439	113.1130
190	6.034080	169.000000	162.965920	.719735	113.3130
191	7.496803	160.000000	152.503197	.704643	113.5130
192	6.473836	149.000000	142.526164	.688285	113.7130
193	8.971522	142.000000	135.028478	.670789	113.9130
194	8.997655	133.000000	124.002345	.652282	114.1130
195	9.561334	125.000000	115.438666	.632897	114.3130
196	9.672825	117.000000	107.327175	.612763	114.5130
197	10.343424	110.000000	99.656576	.592009	114.7130
198	9.585319	102.000000	92.414681	.570760	114.9130
199	9.411468	95.000000	85.588532	.549138	115.1130
200	9.835467	89.000000	79.164533	.527261	115.3130
201	10.871432	84.000000	73.128568	.505240	115.5130
202	10.533889	78.000000	67.466111	.483181	115.7130
203	9.837662	72.000000	62.162338	.461183	115.9130
204	10.797775	68.000000	57.202225	.439338	116.1130
205	10.429360	63.000000	52.570640	.417731	116.3130
206	9.747564	58.000000	48.252436	.396440	116.5130
207	10.767479	55.000000	44.232521	.375535	116.7130
208	10.504061	51.000000	40.495939	.355079	116.9130
209	9.972070	47.000000	37.027930	.335127	117.1130
210	10.186010	44.000000	33.813990	.315728	117.3130
211	9.160077	40.000000	30.839923	.296924	117.5130
212	8.908116	37.000000	28.091884	.278748	117.7130
213	9.443581	35.000000	25.556419	.261228	117.9130
214	8.779501	32.000000	23.220499	.244288	118.1130
215	8.928458	30.000000	21.071542	.228242	118.3130
216	7.902559	27.000000	19.097441	.212801	118.5130
217	7.713425	25.000000	17.286575	.198072	118.7130
218	7.372178	23.000000	15.627822	.184056	118.9130
219	6.889430	21.000000	14.110570	.170749	119.1130
220	7.275285	20.000000	12.724715	.158144	119.3130

NUMBER OF INTEGER WORDS OF STORAGE USED IN PRECEDING PROBLEM 2384
CPU TIME USED 6.661 SECONDS

PAGE 6

BMDPAR--DERIVATIVE-FREE NONLINEAR REGRESSION
EXECUTED ON 83/04/11.AT 21.58.35.

PROGRAM CONTROL INFORMATION

NO MORE CONTROL LANGUAGE.

PROGRAM TERMINATED